ORIGINAL PAPER

Claudin 7 is reduced in uterine epithelial cells during early pregnancy in the rat

Connie E. Poon · Romanthi J. Madawala ·
Margot L. Day · Christopher R. Murphy

Abstract The non-receptive uterine luminal epithelium forms an intact polarised epithelial barrier that is refractory to blastocyst invasion. During implantation, organised dismantling of this barrier leads to a receptive state promoting blastocyst attachment. Claudins are tight junction proteins that increase in the uterine epithelium at the time of implantation. Claudin 7 is a member of this family but demonstrates a basolateral localisation pattern that is distinct from other claudins. The present study investigated the localisation, abundance and hormonal regulation of claudin 7 to elucidate a role for the protein during implantation. The results showed that claudin 7 demonstrates a distinct basal and lateral localisation in the uterine luminal and glandular epithelium throughout early pregnancy. On day 1, claudin 7 is abundantly present in response to ovarian estrogen. At the time of implantation, claudin 7 decreases in abundance. This decrease is not dependent on blastocyst presence, as shown by results in pseudopregnant animals. We propose that claudin 7 mediates intercellular adhesions in the uterine epithelium and also may be responsible for stabilising adhesion proteins at the basolateral cell surface. Thus, claudin 7 may function under the maintenance of the uterine luminal epithelial barrier, in the non-receptive state preventing implantation from occurring.

Keywords Rat · Hormones · Ovariectomy · Uterus · Pseudopregnancy

C. E. Poon (✉) · R. J. Madawala · C. R. Murphy
Cell and Reproductive Biology Laboratory, School of Medical Sciences (Discipline of Anatomy and Histology) and The Bosch Institute, The University of Sydney, N364, F13 Anderson Stuart Building, Sydney, NSW 2006, Australia
e-mail: conniep@anatomy.usyd.edu.au

M. L. Day
School of Medical Sciences (Discipline of Physiology) and The Bosch Institute, The University of Sydney, The Medical Foundation Building, Sydney, NSW 2050, Australia

Introduction

Blastocyst implantation is a delicately orchestrated event that is highly dependent on hormonal and temporal inputs (Carson et al. 2000; Kennedy et al. 2007; Lopata 1996; Psychoyos 1976). A key player is the uterine luminal epithelium which when non-receptive forms a normal intact epithelial barrier that is refractory to invasive elements, including blastocysts (Murphy and Shaw 1994; Psychoyos 1976, 1986; Short and Yoshinaga 1967). During implantation under the conditioning of the ovarian hormones, progesterone and estrogen, this barrier undergoes major structural and morphological changes to form an altered epithelium receptive to blastocyst attachment and subsequent access to the underlying endometrial stroma (Fain et al. 1973; Psychoyos 1976). At the plasma membrane level this process is known as the plasma membrane transformation (Murphy 2004). Understanding the dismantling of the epithelial barrier is an interesting cell biological issue as well as being important to understand the failures in the implantation process and potentially the factors contributing to infertility (Achache and Revel 2006; Fazleabas and Strakova 2002; Haughian et al. 2006).

Tight junctions are a major component in the formation of epithelial barriers (Anderson and Van Itallie 2009; Matter and Balda 2003). These structures form distinct 'kissing points' or 'seals' at the apical portion of the lateral cell membranes between adjacent epithelial cells (Fanning et al.

1999; Tsukita and Furuse 2000). Not only do tight junctions control the diffusion of proteins and molecules between the apical and basolateral cell membranes but also they regulate ion, water and molecular transport through the paracellular space between epithelial cells (Fanning et al. 1999; Tsukita and Furuse 2000). Their apical positioning also enables tight junctions to prevent the entry of invasive organisms and molecules from the apical portion of the epithelium (Tsukita and Furuse 2000; Turksen and Troy 2004). Claudins are a major component of tight junctions and are a family of 22–27 kDa tetraspan transmembrane proteins with at least 24 members, which are integral components of epithelial tight junctions (Turksen and Troy 2004).

In the uterus, at least four claudin proteins, claudins 1, 3, 4 and 5, have been detected in the uterine epithelium during the estrous cycle and early pregnancy (Nicholson et al. 2010; Wang et al. 2004). Two of these, claudin 3 and 4, demonstrate a specific localisation to the tight junction and claudin 4, in particular, demonstrates an upregulation at the time of implantation (Nicholson et al. 2010; Wang et al. 2004). Claudin 4 has been proposed to play a role in decreasing paracellular solute transport by promoting tight adhesions in the tight junction and thus, contributes to the regulation of luminal fluid contents to promote blastocyst implantation (Nicholson et al. 2010; Wang et al. 2004).

Claudin 7 is a protein belonging to the claudin family that is unlike the family's other members in that its localisation is not restricted to epithelial tight junctions (Gonzalez-Mariscal et al. 2006; Inai et al. 2007; Li et al. 2004; Mendoza-Rodriguez et al. 2005). Instead, the protein demonstrates a distinct basolateral localisation in normal epithelia including the murine intestine and nephron and rat epididymis (Amasheh et al. 2011; Ding et al. 2012; Fujita et al. 2006; Gonzalez-Mariscal et al. 2006; Holmes et al. 2006; Inai et al. 2007; Li et al. 2004; Markov et al. 2010; Tatum et al. 2010). Claudin 7 also demonstrates this pattern of staining in rat uterine luminal epithelial cells during the estrous cycle, where interestingly, it is suggested to function outside of tight junctions (Mendoza-Rodriguez et al. 2005).

This finding that claudin 7 is in uterine epithelial cells during the estrous cycle suggests that the protein may also be important during pregnancy, so the present study sought to investigate the localisation pattern and abundance of claudin 7 in the rat uterus during early pregnancy and determine its regulation by ovarian hormones and the blastocyst.

Materials and methods

Animals

Fifty-four virgin Wistar rats of 10–12 weeks of age were used in this study. The animals were maintained under a 12 h light–dark cycle at a temperature of 21 °C and were fed and watered ad libitum.

Pregnant animals

Proestrus females (confirmed by vaginal smears) were mated overnight with a male of proven fertility. Females with spermatozoa present in the vaginal smear taken on the following morning were designated as 'day 1' of pregnancy. A total of 27 pregnant rats (15 for immunofluorescence, 12 for western blotting) were randomly allocated a day of pregnancy (1, 3, 6, 7 or 9) on which killing was to occur. On the day of killing, animals were killed with a 0.25 mL intraperitoneal injection of sodium pentobarbitone (Nembutal; Merial Australia, NSW, Australia) and tissue processed for immunofluorescence and western blotting. All experimental procedures were approved by the University of Sydney Ethics Committee.

Pseudopregnant animals

Proestrus females were mated overnight with a vasectomised male. Pseudopregnancy was confirmed with a vaginal plug the following day and daily vaginal smears to check for an arrested cycle (Swingle et al. 1951). Three pseudopregnant animals were killed on day 6 of pseudopregnancy in the same method as for pregnant animals above.

Pregnant tissue collection

For immunofluorescence analysis, tissue from 15 pregnant rats was collected on days 1, 3, 6, 7 and 9 of pregnancy (three rats per day of pregnancy). Uterine horns were excised, cut into 5 mm sections and embedded in O.C.T. medium (Tissue Tek; Sakura Finetek, Torrence, CA, USA) followed by immersion in super-cooled isopentane (BDH Laboratory Supplies, Poole, England). Tissue was then frozen and stored until use in liquid nitrogen. For western blotting, tissue from 12 pregnant rats on days 1, 3, 6 and 7 of pregnancy (three rats per day of pregnancy), uterine horns were excised, cut longitudinally to expose the epithelium. The complete luminal epithelial surface for all animals was removed by gentle scraping using sterile surgical blades and placed immediately in cold lysis buffer (50 mM Tris–HCl, 1 mM EDTA, 150 mM NaCl, 0.5 % SDS, 2.5 % DOC, 5 % Igepal, 1 % protease inhibitor cocktail; Sigma, Saint Louis Missouri, USA) as described previously and according to the manufacturer's instructions (Kaneko et al. 2008; Nicholson et al. 2010). The epithelial cell suspension was then passed through a 23-gauge needle using a 1 mL syringe (Livingstone International, Rosebury, NSW, Australia) and briefly centrifuged at 8,000g at 4 °C for 3 min. The supernatant was carefully removed and then

585

frozen in liquid nitrogen in 5 µl aliquots and stored at −80 °C for subsequent use.

Pseudopregnant tissue collection

For immunofluorescence analysis, tissue from three pseudopregnant rats was collected on day 6 of pseudopregnancy. Four 3 mm tissue pieces were cut from both uterine horns of each rat and were processed separately for immunofluorescence analysis as for pregnant tissue above. The remainder of each uterine horn for each pseudopregnant rat was processed for western blotting analysis as for pregnant tissue above.

Ovariectomy

Bilateral ovariectomy on 24 rats was performed under anaesthesia with an intraperitoneal injection of xylazine (4 mg/kg; TROY laboratories Pty. Ltd., Smithfield, NSW, Australia) and ketamine (75 mg/kg; Parrell Laboratories (AUST) Pty. Ltd., Alexandria, NSW, Australia). Animals were monitored and allowed to recover for 3 weeks. Progesterone (Sigma, USA) and 17-β-oestradiol (Sigma) were dissolved using benzyl alcohol (Sigma) and peanut oil (1:4 v/v) (carrier) and administered via subcutaneous injection in the scruff of the neck as previously described (Murphy and Rogers, 1981). Rats were then randomly allocated to one of the following treatment groups (six rats per treatment group) and injected over three consecutive days: Group 1 (control) injected with 0.1 mL of carrier only (benzyl alcohol and peanut oil); Group 2 (estrogen only) injected with 0.1 mL of estrogen (0.5 mg); Group 3 (progesterone only) injected with 0.1 mL of progesterone (5 mg); Group 4 (progesterone and estrogen) injected with 0.1 mL of progesterone (5 mg) for three days and on the third day received an additional injection of 0.1 mL of estrogen (0.5 mg). After the final injection, the rats were left for 24 h before killing and tissue was collected from 12 rats (three per treatment group) for immunofluorescence and the remaining 12 rats (three per treatment group) for western blotting analysis, as described above.

Immunofluorescence

Frozen sections of pregnant and pseudopregnant uterine horns were cut (7 µm thickness) and transferred to gelatine–chrome alum-coated slides using a Leica CM3050 cryostat (Leica, Heerbrugg, Switzerland). Sections were then fixed in 100 % acetone (Biolab Australia, Mulgrave, VIC, Australia) for 15 min, and blocked using 1 % bovine serum albumin (BSA) in phosphate buffered saline (PBS) for 30 min. Sections were probed with 0.66 µg/mL of primary antibody (goat anti-claudin 7 antibody, Santa Cruz

Biotechnology, Inc., USA) overnight at 4 °C and washed 3 × 5 min in PBS. The sections were then incubated with 20 µg/mL donkey anti-goat secondary antibody conjugated to Alexa 488 (Invitrogen, Mulgrave, VIC, Australia), followed by 3 × 5 min washes in PBS. Sections were then mounted and coverslipped using 25 µl of Vectashield mounting medium with DAPI (Vector Laboratories, Burlingame, CA, USA) and examined with the Zeiss Deconvolution microscope (Carl Zeiss Pty. Ltd., Australasia, North Ryde, NSW Australia) using the reflected light filters: DAPI (365, 395LP, 420LP) and Alexa 488 (480/40, 505LP, 535/50). Images were captured using a Zeiss AxioCam HR digital monochrome CCD camera (Carl Zeiss Pty. Ltd.) and analysed using the Zeiss AxioVision version 4.0 image acquisition software. Non-specific immunoglobulin (IgG) serum antibody (Sigma) controls were additionally processed along with experimental sections to determine specificity of the secondary antibody.

Western blot

Protein concentrations of isolated epithelial cell lysate were determined by a BCA protein assay (MicroBCA™ Protein assay kit; Quantum Scientific, Murarrie, QLD, Australia) and POLARstar microplate reader (BMG LabTech, Durham, NC, USA), according to the manufacturer's instructions. Protein samples were subjected to SDS-PAGE on a 15 % resolving acrylamide gel. A total of 20 µg of protein with sample buffer (8 % glycerol, 50 mM Tris–HCl (pH 6.8), 1.6 % SDS, 0.024 % bromophenol blue, 4 % β-mercaptoethanol) was loaded immediately (without boiling) into each well of the gel and run at 200 V for 45 min. Gels were subsequently transferred (100 V for 1 h and 45 min) to Immobilon™ PVDF membranes (Millipore, Bedford, MA, USA). Membranes were then blocked using filtered 5 % skim milk powder diluted in TBST (10 mM Tris–HCl (pH 7.4), 150 mM NaCl and 0.05 % Tween 20) for 1 h at room temperature and under gentle agitation. After blocking, membranes were incubated with primary antibody (goat anti-claudin 7 antibody, Santa Cruz Biotechnology, Inc., USA) at a concentration of 0.1 µg/mL diluted in 1 % skim milk in TBST overnight at 4 °C on a rocking platform. Membranes were then rinsed in TBST, 3 × 10 min and incubated with secondary antibody (rabbit anti-goat IgG polyclonal horseradish peroxidase-linked, Dako, Glostrup, Denmark) diluted in 1 % skim milk powder in TBST for 2 h at room temperature with gentle agitation. Membranes were subsequently rinsed 3 × 10 min with TBST. Protein bands on the membranes were visualised using the Immobilon Western HRP Substrate (Millipore, Bedford, MA, USA) and captured using a CCD camera and the Bio-Rad ChemiDoc MP System (Bio-Rad Laboratories, NSW, Australia). Image analysis was conducted using the Bio-Rad Image Lab 4.0

Fig. 1 Claudin 7 protein localisation in rat uterine luminal epithelial cells (UECs) during normal pregnancy. Single channel (Alexa 488 only) (**a, c, e, g, i, k**) and double channel (Alexa 488 and DAPI) (**b, d, f, h, j, l**) immunofluorescence micrographs of UECs stained for claudin 7 protein (Alexa 488, *green*) and nuclei (DAPI, *blue*) on day 1 (**a, b**), day 3 (**c, d**), day 6 (**e, f**), day 7 (**g, h**) and day 9 (**i, j**) of normal pregnancy, with representative non-immune controls of day 1 of pregnancy (**k, l**). Images are representative of staining obtained from three separate experiments. *U* uterine luminal epithelium, *arrow* apical cell surface. *Scale bar* 20 µm
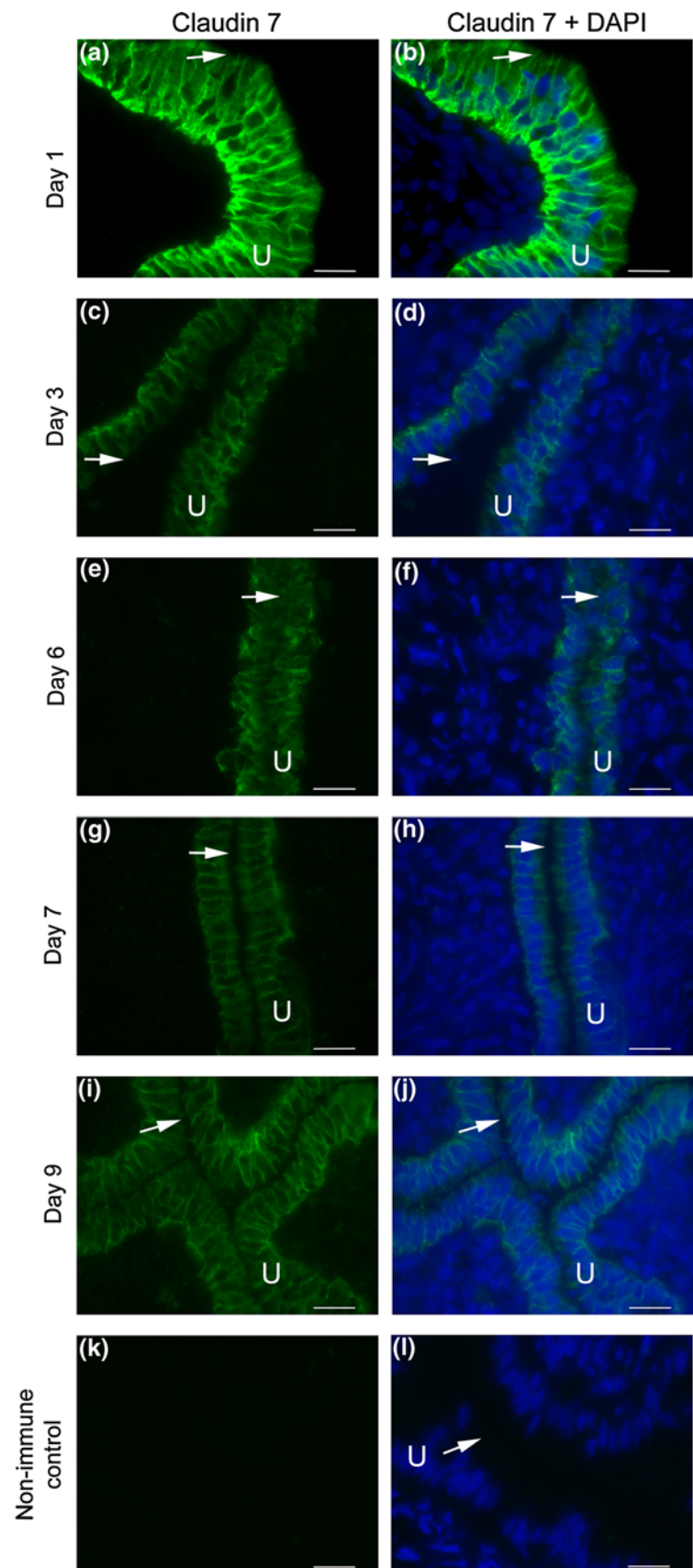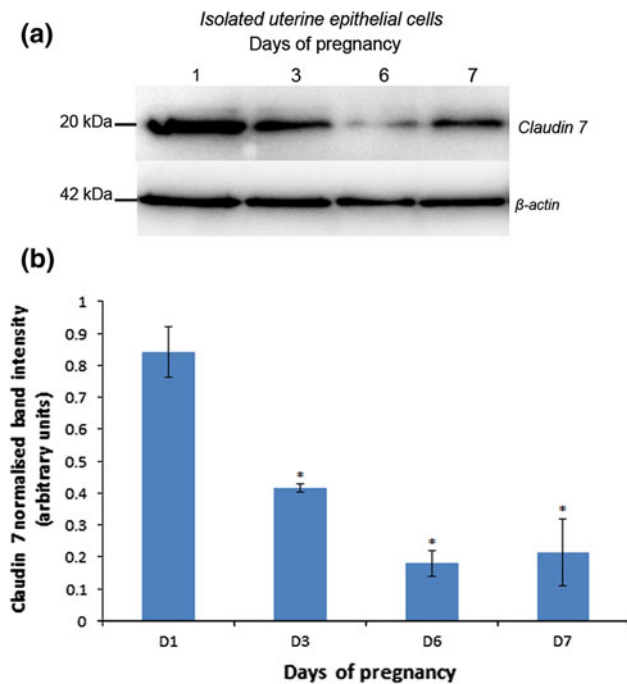
(a) Western blotting of claudin 7 protein in isolated rat luminal epithelial cells from days 1, 3, 6 and 7 of early pregnancy. β-Actin was used as a loading control. **b** Densitometric and statistical analysis (ANOVA and Tukey's post hoc test) of western blotting was performed. *Each bar* is the mean ± SEM, $n = 3$ separate experiments. *Significant difference to day 1 of pregnancy ($p < 0.05$, $n = 3$)

software (Bio-Rad). To confirm equal protein loading, membranes were stripped using heating at 60 °C for 45 min in stripping buffer (62.5 mM Tris–HCl (pH6.7), 2 % SDS and 100 mM β-mercaptoethanol) and reprobed with mouse monoclonal anti β-actin antibody (Sigma) at a concentration of 1 μg/mL as per the method used for the primary antibody. The secondary antibody for β-actin (sheep anti-mouse IgG polyclonal horseradish peroxidase-linked antibody, Dako, Glostrup, Denmark) was used at a concentration of 0.47 μg/mL. Membranes were visualised and analysed as per the procedure above.

Densitometry

The intensity of the bands detected from western blotting analysis was quantified using the Volume Analysis Tool from the Bio-Rad Image Lab 4.0 software (Bio-rad). Intensity volumes were then normalised to β-actin volume intensity values followed by statistical analysis of the adjusted normalised intensity volumes. Statistical analysis was conducted with IBM SPSS Statistics Data Editor (Version 20, New York, United States) using one-way ANOVA and Tukey's post hoc test ($p < 0.05$ was considered significant). The mean ± SEM was then calculated for all data and bar graphs were formed using Microsoft Excel.

Results

Claudin 7 protein is localised to the basal and lateral cell surfaces of the luminal and glandular epithelium during early pregnancy

Immunofluorescence was used to localise claudin 7 protein in the rat endometrium during days 1, 3, 6, 7 and 9 of early pregnancy. On day 1 of pregnancy, strong staining for claudin 7 was present along the basal and lateral cell surfaces of the luminal and glandular epithelia (not shown) but notably absent in the underlying stroma (Fig. 1a, b). In some cells, the protein was distinctly concentrated towards the basal portion of the cells, underlying the nucleus. On days 3, 6, 7 and 9 (Fig. 1c–j) of pregnancy, claudin 7 protein expression was markedly decreased when compared to day 1. The protein retained its localisation to the basal and lateral membranes; however, on days 7 and 9, there was also diffuse claudin 7 staining in the apical region of the cytoplasm (Fig. 1g–j). All non-immune controls were negative for staining (Fig. 1k, l).

Claudin 7 protein expression decreases during early pregnancy

Claudin 7 protein was present in uterine epithelial cells isolated from days 1, 3, 6 and 7 of early pregnancy as demonstrated by western blotting analysis. Claudin 7 was present as a 20 kDa band which decreased in intensity from day 1 through days 3 and 6 of pregnancy (Fig. 2a). Equal loading of protein samples was confirmed with β-actin. Densitometric analysis revealed there was a statistically significant decrease in the amount of claudin 7 protein on days 3, 6 and 7 when compared with day 1 of pregnancy in isolated uterine epithelial cells ($p < 0.05$, $n = 3$ per day) (Fig. 2b).

Claudin 7 protein is abundant at the basal cell surface of the luminal epithelium under the influence of estrogen alone

Immunofluorescence and western blotting were used to localise and measure the abundance, respectively, of claudin 7 in the rat endometrium in ovariectomised rats. Ovariectomy was used to determine the hormonal regulation profile of claudin 7. The vehicle-treated group demonstrated relatively uniform claudin 7 protein localisation at the basal and lateral cell borders (Fig. 3a, b). In response to estrogen, claudin 7 was localised to the basal and lateral cell surfaces of the luminal epithelium, with the protein concentrated towards the basal portion of the cells, underlying the nucleus (Fig. 3c, d). This result was comparable to that obtained on day 1 of pregnancy. Both

Fig. 3 Claudin 7 protein localisation in rat uterine luminal epithelial cells (UECs) from ovariectomised and hormone supplemented rats. Single channel (Alexa 488 only) (**a**, **c**, **e**, **g**, **j**) and double channel (Alexa 488 and DAPI) (**b**, **d**, **f**, **h**, **k**) immunofluorescence micrographs of UECs stained for claudin 7 protein (Alexa 488, *green*) and nuclei (DAPI, *blue*) from rats treated with vehicle alone (**a**, **b**), estrogen alone (**c**, **d**), progesterone alone (**e**, **f**), and progesterone and estrogen combined (**g**, **h**) with representative non-immune controls of estrogen-treated rats (**j**, **k**). Images are representative of staining obtained from three separate experiments. *U* uterine luminal epithelium, *arrow* apical cell surface. *Scale bar* 20 μm
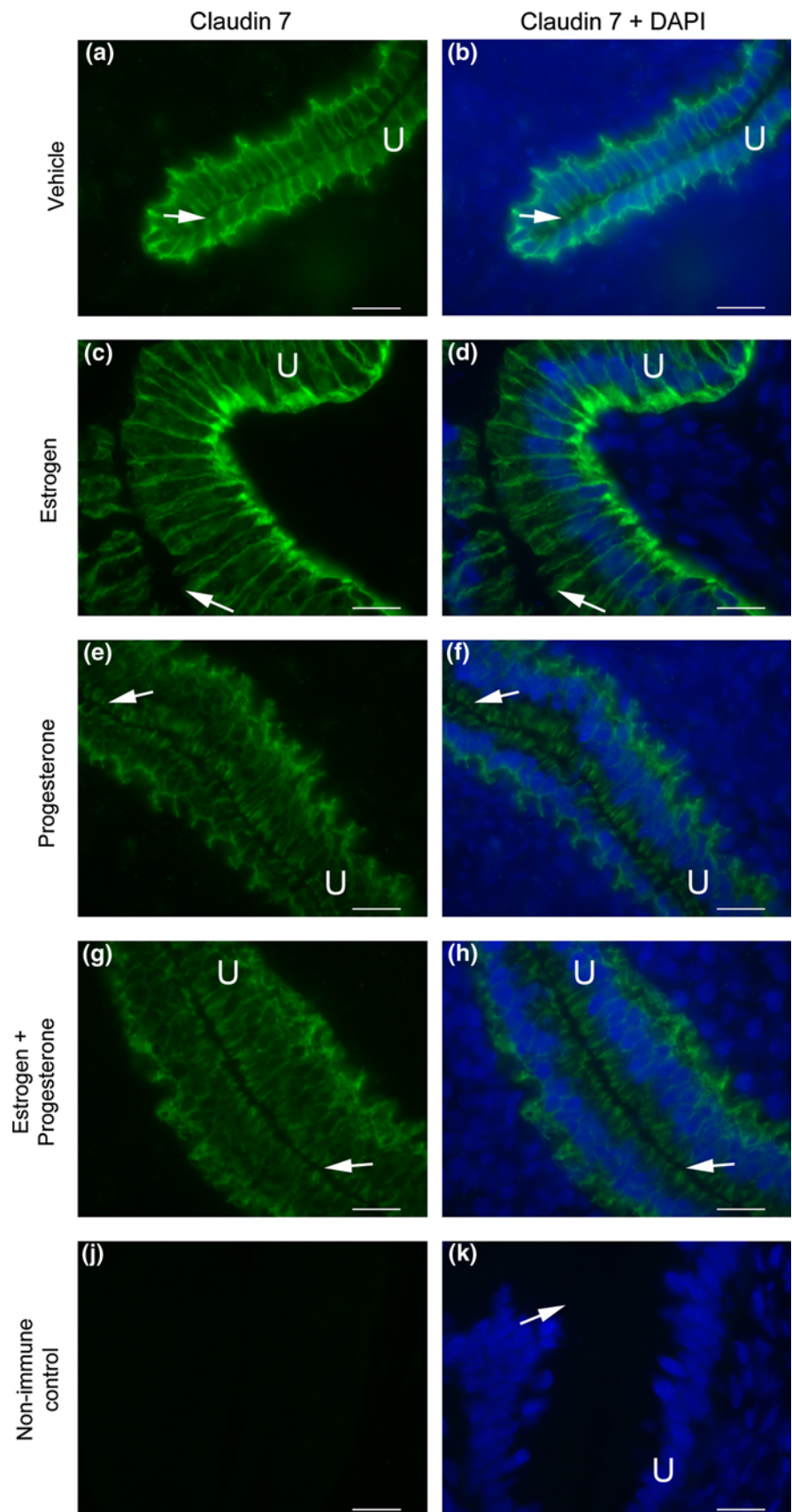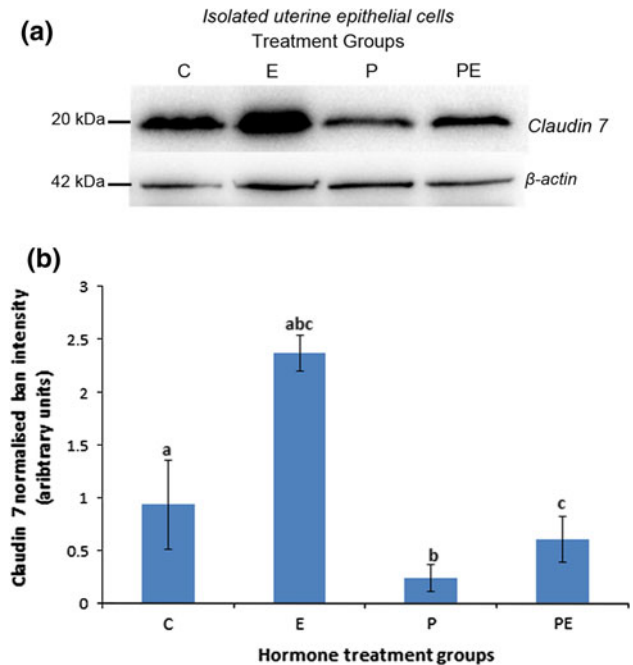
progesterone alone and progesterone in combination with estrogen produced similar levels and patterns of staining with faint claudin 7 staining localised to the basolateral cell surfaces. As observed in sections from days 7 and 9 of pregnancy, there was also diffuse staining for claudin 7 in the apical region of the cell cytoplasm (Fig. 3e–h). The accumulation of claudin 7 protein at the basal portion of the cells as seen in estrogen-treated rats was absent in the progesterone alone and progesterone plus estrogen-treated rats (Fig. 3e–h). All non-immune controls were negative for staining (Fig. 3j, k). Western blotting analysis confirmed the immunofluorescence results, with a greater amount of claudin 7 protein being present in the estrogen treated group compared with the vehicle-treated group (Fig. 4, $p < 0.05$, $n = 3$ per treatment). In the progesterone alone and progesterone plus estrogen treated groups the amount of claudin 7 protein was decreased when compared with the estrogen treated group but were not different to the vehicle control group.

The decreased levels of claudin 7 protein on day 6 are due to maternal factors and are independent of blastocyst presence

Pseudopregnancy was used to confirm that the decrease in claudin 7 protein at the time of implantation was not dependent on the presence of the blastocyst. On day 6 of pseudopregnancy, claudin 7 demonstrated a low level of basolateral staining in the luminal epithelium and was present at comparable levels to that observed on day 6 of pregnancy (Fig. 5a–d), but at a lower level than on day 1 of pregnancy (Fig. 5e, f). All non-immune controls were negative for staining (Fig. 5g, h). Western blotting analysis further demonstrated that uterine luminal epithelial cells taken from day 6 pseudopregnant animals exhibited comparable levels of claudin 7 expression to day 6 pregnant animals (Fig. 6a). There was significantly less claudin 7 protein in lysates from both day 6 pregnant and day 6 pseudopregnant rats compared with day 1 pregnant animals (Fig. 6b), whereas there was no significant difference in claudin 7 protein levels between day 6 pseudopregnant and day 6 pregnant animals ($p > 0.05$, $n = 3$).

Discussion

The transition to uterine receptivity is dependent on the dismantling of the tight uterine luminal epithelial barrier in preparation for blastocyst invasion (Murphy 2004). The process involves a restructuring of the intercellular adhesions in the lateral membrane and the basal cell membrane to the underlying extracellular matrix such that the uterine epithelial cells downregulate intercellular adhesions,


Fig. 4 **a** Western blotting of claudin 7 protein in isolated rat luminal epithelial cells from ovariectomised rats treated with vehicle alone (C), estrogen alone (E), progesterone alone (P) and progesterone and estrogen combined (PE). β-Actin was used as a loading control. **b** Densitometric and statistical analysis (ANOVA and Tukey's post hoc test) of western blotting was performed. *Bars* with the same letter are significantly different ($p < 0.05$, $n = 3$). *Each bar* is the mean ± SEM, $n = 3$ separate experiments

detach from the basal lamina and permit the blastocyst access to the underlying endometrial stroma (Illingworth et al. 2000; Kaneko et al. 2011; Li et al. 2002; Murphy 2000a, 2004). The present work suggests that claudin 7 is a new player in this process.

In the non-receptive uterus under the control of estrogen, claudin 7 is abundant at the basolateral cell surfaces of the uterine luminal epithelial as a 20 kDa protein. At the time of implantation on day 6, while claudin 7 retains a basolateral localisation, the levels of protein decrease in a process independent of blastocyst presence, as demonstrated by its occurrence in pseudopregnant animals. The decrease in claudin 7 was also not attributable to the combined activity of progesterone and estrogen as demonstrated in the ovariectomy study which raises the possibility of regulation by factors contained in seminal fluid, which are known to promote receptivity and implantation in rodents (Carp et al. 1984; Robertson 2007).

While this is the first study of claudin 7 in the rat uterus during early pregnancy, claudin 7 has been documented in the rat uterus during the estrous cycle, where the protein demonstrated a similar basolateral pattern of localisation (Mendoza-Rodriguez et al. 2005). There was confinement of the protein to the low lateral and basal portion of the cells during the estrous stage of the cycle which was

Fig. 5 Claudin 7 protein localisation in rat uterine luminal epithelial cells (UECs) during day 6 pseudopregnancy and day 1 and day 6 of normal pregnancy. Single channel (Alexa 488 only) (**a, c, e, g**) and double channel (Alexa 488 and DAPI) (**b, d, f, h**) immunofluorescence micrographs of UECs stained for claudin 7 protein (Alexa 488, *green*) and nuclei (DAPI, *blue*) on day 6 of pseudopregnancy (**a, b**) and day 6 (**c, d**) and day 1 (**e, f**) of normal pregnancy, with representative non-immune controls on day 6 of pseudopregnancy (**g, h**). Images are representative of staining obtained from three separate experiments. *U* uterine luminal epithelium, *arrow* apical cell surface. *Scale bar* 20 μm
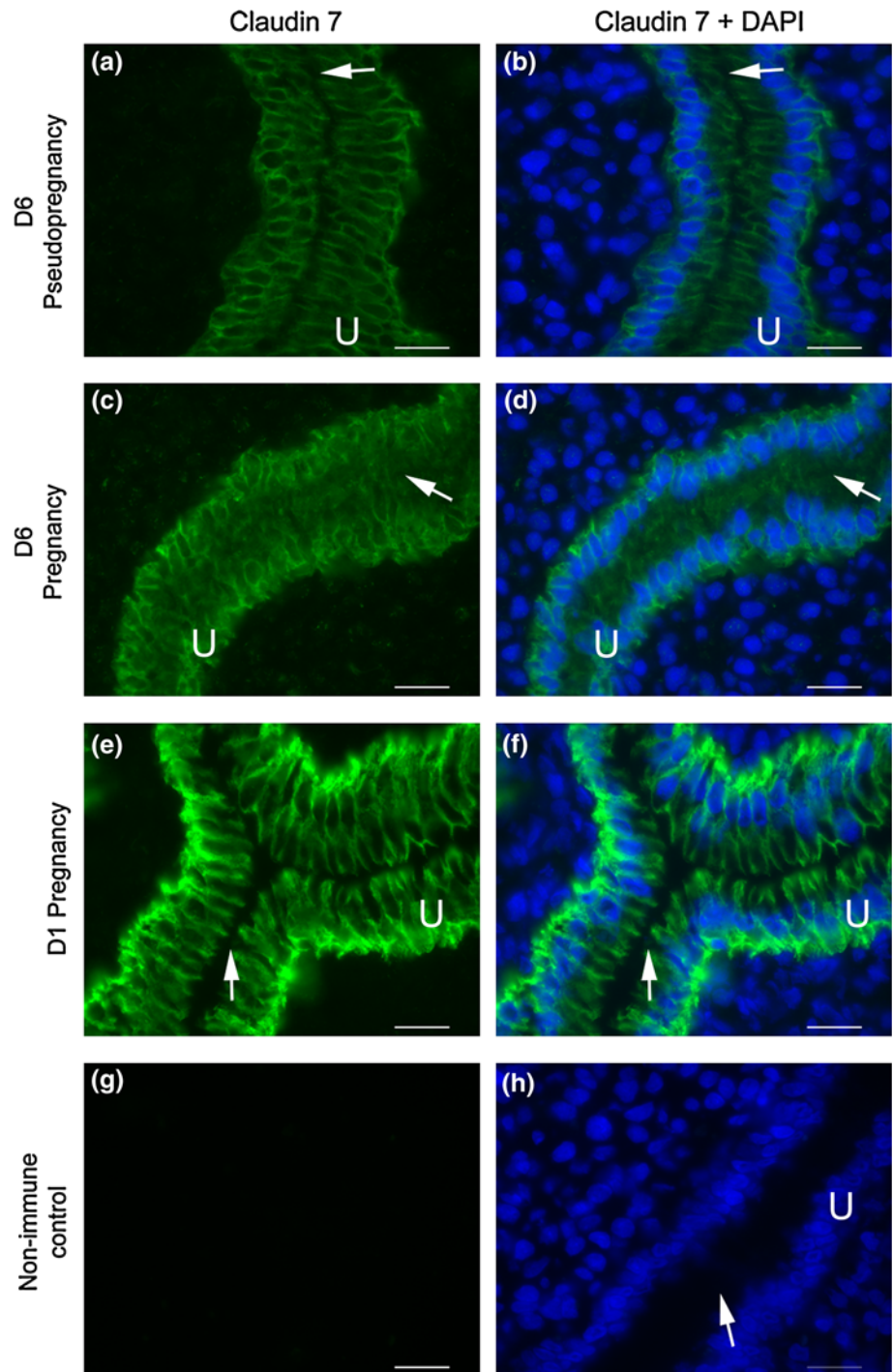

suggested to be under combined activity of progesterone and estrogen (Mendoza-Rodriguez et al. 2005). This result is consistent with the present work which found that on day 6 of pregnancy there is a similar localisation.

The basolateral pattern of staining of claudin 7 protein we saw is common to a variety of other epithelial tissues including the intestine, mammary gland, kidney and epididymis and claudin 7, like other claudin proteins, has been suggested to mediate intercellular adhesions (Amasheh

et al. 2011; Ding et al. 2012; Fujita et al. 2006; Gonzalez-Mariscal et al. 2006; Holmes et al. 2006; Inai et al. 2007; Markov et al. 2010). In contrast to other claudins, however, which are usually localised only to the epithelial tight junctions, claudin 7 appears to mediate adhesion outside tight junctions, that is, along the length of the lateral cell border and perhaps even along the basal cell border with the underlying extracellular matrix, as suggested by the basolateral protein location (Angelow et al. 2008;
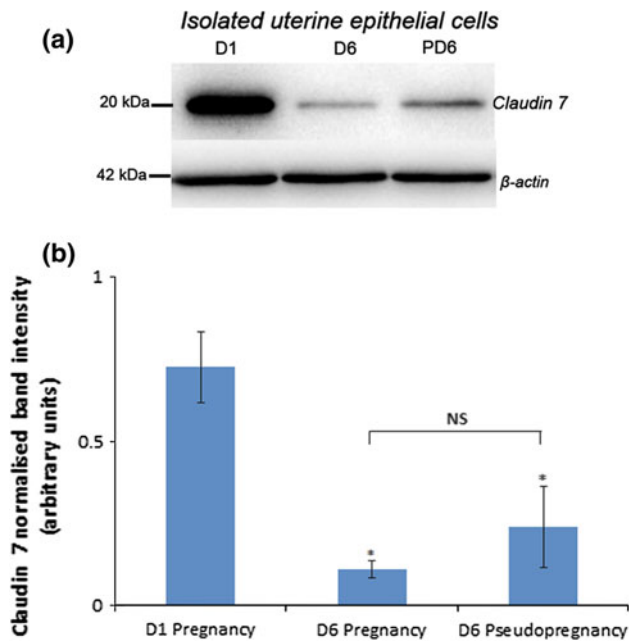
Fig. 6 **a** Western blotting of claudin 7 protein in isolated rat luminal epithelial cells from day 6 of pseudopregnancy (PD6) and days 1 (D1) and 6 (D6) of pregnancy. β-Actin was used as a loading control. **b** Densitometric and statistical analysis (ANOVA and Tukey's post hoc test) of western blotting was performed. *Each bar* is the mean ± SEM, $n = 3$ separate experiments. *Significant difference to D1 pregnancy ($p < 0.05$), *NS* not significant ($p > 0.05$)

Ding et al. 2012; Inai et al. 2007; Li et al. 2004) which we also saw.

In the uterus on day 6 of pregnancy, uterine epithelial cells lose both focal adhesions in the basal plasma membrane and desmosomes along the lateral cell borders producing a loosely adhered epithelial barrier (Illingworth et al. 2000; Kaneko et al. 2009; Kaneko et al. 2008; Preston et al. 2006; Tinel et al. 2000). The decrease in claudin 7 at the basolateral borders shown here at the time of implantation adds to our understanding of this process and supports the hypothesis that the protein is serving an intercellular and cell–matrix adhesive function. Our finding that estrogen after progesterone produces no further reduction in claudin 7 over that seen with progesterone alone is consistent with findings on other basolateral proteins, which are not further reduced by estrogen after progesterone (Kaneko et al. 2011; Kaneko et al. 2009; Kaneko et al. 2008; Murphy 2000b, 2004).

It would be interesting to investigate the mechanism by which claudin 7 promotes this cell–matrix adhesion. Claudin 7 knockout in murine intestine was observed to result in severe disruption of the mucosal integrity due to the absence of the structural intercellular adhesions mediated by the protein in the intestinal epithelium (Ding et al. 2012; Tatum et al. 2010). Further, a disruption to the

integrity of integrin α2 was observed with claudin 7 knockout, suggesting that the mechanism by which claudin 7 promotes cell–matrix adhesion is via stabilising integrin α2 proteins which themselves are responsible for attachment to extracellular matrix components (Ding et al. 2012). It would be interesting to determine if claudin 7 is acting by a similar mechanism in the rat endometrium during early pregnancy and is responsible for maintaining an intact uterine epithelial barrier during the non-receptive phase, preventing implantation from occurring.

In addition to promoting intercellular and cell–matrix adhesions, claudin 7 has also been linked to the regulation of paracellular transport. In LLC-PK1 cells, overexpression of claudin 7 decreases Cl^- and increases Na^+ paracellular conductance (Johnson et al. 2005). Further, mice with claudin 7 knockout demonstrated significant chronic dehydration and growth retardation caused by Na^+, Cl^- and K^+ wasting in the renal tubular epithelial cells (Tatum et al. 2010). The authors concluded that claudin 7 was essential for the maintenance of ionic homeostasis (Tatum et al. 2010).

In the non-pregnant rat uterus, claudin 7 may be functioning in this capacity, however, it has been found in the mouse uterus that the concentration of Na^+ in uterine secretions double around 18 h prior to the implantation (Van Winkle et al. 1983). Thus, it does not seem likely that claudin 7 is serving this function of increasing paracellular Na^+ conductance, given its decrease in the uterine luminal epithelial cells in the peri-implantation period.

In summary, the present study established that claudin 7 was present in the rat endometrium during pregnancy and is localised to the uterine luminal and glandular epithelium during early pregnancy. The results suggest that claudin 7 acts as an adhesion molecule that facilitates adhesion between adjacent uterine epithelial cells as well as between uterine epithelial cells and the underlying basal lamina. We further show that claudin 7 protein is drastically reduced as pregnancy progresses toward uterine receptivity for blastocyst implantation and we suggest that this is a further contribution to the plasma membrane transformation (Murphy 2004), which sees uterine luminal epithelial cells detach from the underlying connective tissue.

References

Achache H, Revel A (2006) Endometrial receptivity markers, the journey to successful embryo implantation. Hum Reprod Update 12:731–746

Amasheh S, Fromm M, Günzel D (2011) Claudins of intestine and nephron—a correlation of molecular tight junction structure and barrier function. Acta Physiol 201:133–140

Anderson JM, Van Itallie CM (2009) Physiology and function of the tight junction. Cold Spring Harb Perspect Biol 1:a002584

Angelow S, Ahlstrom R, Yu AS (2008) Biology of claudins. Am J Physiol Renal Physiol 295:F867–F876

Carp HJ, Serr DM, Mashiach S, Nebel L (1984) Influence of insemination on the implantation of transferred rat blastocysts. Gynecol Obstet Invest 18:194–198

Carson DD, Bagchi I, Dey SK, Enders AC, Fazleabas AT, Lessey BA, Yoshinaga K (2000) Embryo implantation. Dev Biol 223: 217–237

Ding L, Lu Z, Foreman O, Tatum R, Lu Q, Renegar R, Cao J, Chen YH (2012) Inflammation and disruption of the mucosal architecture in claudin-7-deficient mice. Gastroenterology 142:305–315

Fain JN, Psychoyos S, Czernik AJ, Frost S, Cash WD (1973) Indomethacin, lipolysis, and cyclic AMP accumulation in white fat cells. Endocrinology 93:632–639

Fanning AS, Mitic LL, Anderson JM (1999) Transmembrane proteins in the tight junction barrier. J Am Soc Nephrol 10:1337–1345

Fazleabas AT, Strakova Z (2002) Endometrial function: cell specific changes in the uterine environment. Mol Cell Endocrinol 186: 143–147

Fujita H, Chiba H, Yokozaki H, Sakai N, Sugimoto K, Wada T, Kojima T, Yamashita T, Sawada N (2006) Differential expression and subcellular localization of claudin-7, -8, -12, -13, and -15 along the mouse intestine. J Histochem Cytochem 54: 933–944

Gonzalez-Mariscal L, Namorado Mdel C, Martin D, Sierra G, Reyes JL (2006) The tight junction proteins claudin-7 and -8 display a different subcellular localization at Henle's loops and collecting ducts of rabbit kidney. Nephrol Dial Transplant 21:2391–2398

Haughian JM, Jackson TA, Koterwas DM, Bradford AP (2006) Endometrial cancer cell survival and apoptosis is regulated by protein kinase C alpha and delta. Endocr Relat Cancer 13:1251–1267

Holmes JL, Van Itallie CM, Rasmussen JE, Anderson JM (2006) Claudin profiling in the mouse during postnatal intestinal development and along the gastrointestinal tract reveals complex expression patterns. Gene Expr Patterns 6:581–588

Illingworth IM, Kiszka I, Bagley S, Ireland GW, Garrod DR, Kimber SJ (2000) Desmosomes are reduced in the mouse uterine luminal epithelium during the preimplantation period of pregnancy: a mechanism for facilitation of implantation. Biol Reprod 63: 1764–1773

Inai T, Sengoku A, Hirose E, Iida H, Shibata Y (2007) Claudin-7 expressed on lateral membrane of rat epididymal epithelium does not form aberrant tight junction strands. Anat Rec (Hoboken) 290:1431–1438

Johnson AH, Frierson HF, Zaika A, Powell SM, Roche J, Crowe S, Moskaluk CA, El-Rifai W (2005) Expression of tight-junction protein claudin-7 is an early event in gastric tumorigenesis. Am J Pathol 167:577–584

Kaneko Y, Lindsay LA, Murphy CR (2008) Focal adhesions disassemble during early pregnancy in rat uterine epithelial cells. Reprod Fertil Dev 20:892–899

Kaneko Y, Lecce L, Murphy CR (2009) Ovarian hormones regulate expression of the focal adhesion proteins, talin and paxillin, in rat uterine luminal but not glandular epithelial cells. Histochem Cell Biol 132:613–622

Kaneko Y, Lecce L, Day ML, Murphy CR (2011) Beta(1) and beta(3) integrins disassemble from basal focal adhesions and beta(3) integrin is later localised to the apical plasma membrane of rat uterine luminal epithelial cells at the time of implantation. Reprod Fertil Dev 23:481–495

Kennedy TG, Gillio-Meina C, Phang SH (2007) Prostaglandins and the initiation of blastocyst implantation and decidualization. Reproduction 134:635–643

Li Q, Wang J, Armant DR, Bagchi MK, Bagchi IC (2002) Calcitonin down-regulates E-cadherin expression in rodent uterine epithelium during implantation. J Biol Chem 277: 46447–46455

Li WY, Huey CL, Yu AS (2004) Expression of claudin-7 and -8 along the mouse nephron. Am J Physiol Renal Physiol 286:F1063–F1071

Lopata A (1996) Blastocyst-endometrial interaction: an appraisal of some old and new ideas. Mol Hum Reprod 2:519–525

Markov AG, Veshnyakova A, Fromm M, Amasheh M, Amasheh S (2010) Segmental expression of claudin proteins correlates with tight junction barrier properties in rat intestine. J Comp Physiol [B] 180:591–598

Matter K, Balda MS (2003) Signalling to and from tight junctions. Nat Rev Mol Cell Biol 4:225–236

Mendoza-Rodriguez CA, Gonzalez-Mariscal L, Cerbon M (2005) Changes in the distribution of ZO-1, occludin, and claudins in the rat uterine epithelium during the estrous cycle. Cell Tissue Res 319:315–330

Murphy CR (2000a) Junctional barrier complexes undergo major alterations during the plasma membrane transformation of uterine epithelial cells. Hum Reprod 15(Suppl 3):182–188

Murphy CR (2000b) The plasma membrane transformation of uterine epithelial cells during pregnancy. J Reprod Fertil Suppl 55:23–28

Murphy CR (2004) Uterine receptivity and the plasma membrane transformation. Cell Res 14:259–267

Murphy CR, Rogers AW (1981) Effects of ovarian hormones on cell membranes in the rat uterus. III. The surface carbohydrates at the apex of the luminal epithelium. Cell Biophys 3:305–320

Murphy CR, Shaw TJ (1994) Plasma membrane transformation: a common response of uterine epithelial cells during the peri-implantation period. Cell Biol Int 18:1115–1128

Nicholson MDO, Lindsay LA, Murphy CR (2010) Ovarian hormones control the changing expression of claudins and occludin in rat uterine epithelial cells during early pregnancy. Acta Histochem 112:42–52

Preston AM, Lindsay LA, Murphy CR (2006) Desmosomes in uterine epithelial cells decrease at the time of implantation: an ultrastructural and morphometric study. J Morphol 267:103–108

Psychoyos A (1976) Hormonal control of uterine receptivity for nidation. J Reprod Fertil Suppl 25:17–28

Psychoyos A (1986) Uterine receptivity for nidation. Ann N Y Acad Sci 476:36–42

Robertson SA (2007) Seminal fluid signaling in the female reproductive tract: lessons from rodents and pigs. J Anim Sci 85:E36–E44

Short RV, Yoshinaga K (1967) Hormonal influences on tumor growth in the uterus of the rat. J Reprod Fertil 14:287–293

Swingle WW, Seay P, Perlmutt J, Collins EJ, Barlow G Jr, Fedor EJ (1951) An experimental study of pseudopregnancy in rat. Am J Physiol 167:586–592

Tatum R, Zhang Y, Salleng K, Lu Z, Lin JJ, Lu Q, Jeansonne BG, Ding L, Chen YH (2010) Renal salt wasting and chronic dehydration in claudin-7-deficient mice. Am J Physiol Renal Physiol 298:F24–F34

Tinel H, Denker HW, Thie M (2000) Calcium influx in human uterine epithelial RL95-2 cells triggers adhesiveness for trophoblast-like cells. Model studies on signalling events during embryo implantation. Mol Hum Reprod 6:1119–1130

Tsukita S, Furuse M (2000) The structure and function of claudins, cell adhesion molecules at tight junctions. Ann N Y Acad Sci 915:129–135

Turksen K, Troy TC (2004) Barriers built on claudins. J Cell Sci 117:2435–2447

Van Winkle LJ, Campione AL, Webster DP (1983) Sodium ion concentrations in uterine flushings from "implanting" and "delayed implanting" mice. J Exp Zool 226:321–324

Wang X, Matsumoto H, Zhao X, Das SK, Paria BC (2004) Embryonic signals direct the formation of tight junctional permeability barrier in the decidualizing stroma during embryo implantation. J Cell Sci 117:53–62